

EC-HEP-950726

Di-photon + Jet Event Structure

B. Bailey

Department of Physics, Eckerd College, Saint Petersburg, Florida 33733

(July 26, 1995)

Abstract

New distributions are presented which allow di-photon + jet events to be clearly separated into three classes of events based on the p_T of the final state particles and their separation $R = \sqrt{(\Delta y)^2 + (\Delta\phi)^2}$. The analysis used can easily be extended to the case of di-jet + photon.

A recent calculation of di-jet + photon suggested a method of separating these events into three classes based on whether the photon had the highest, middle or lowest energy fraction [1]. I refer the interested reader to Ref. [1] and references contained therein. The analysis here uses different observables and distributions. The cuts necessary are simple and the observables may be constructed from the four-vectors of the final state particles in the lab (hadron-hadron center-of-momentum) frame.

The di-photon + jet cross section consists of, at the Born level, $q\bar{q} \rightarrow \gamma\gamma g$, $qg \rightarrow \gamma\gamma q$ and $\bar{q}g \rightarrow \gamma\gamma\bar{q}$. In this brief note it will be shown that by ordering events by the p_T of the jet, and looking at experimentally motivated distributions, that di-photon + jet events can be clearly separated into three classes. These three classes are: (1) $p_{Tjet} > p_{T\gamma 1} > p_{T\gamma 2}$, (2) $p_{T\gamma 1} > p_{Tjet} > p_{T\gamma 2}$, and (3) $p_{T\gamma 1} > p_{T\gamma 2} > p_{Tjet}$. The distributions in question are motivated by the cone algorithm, $R = \sqrt{(\Delta y)^2 + (\Delta\phi)^2}$, used to define jets and isolated photons. Where Δy is the magnitude of the difference in rapidity of two final state particles and $\Delta\phi$ is the azimuthal opening angle between the two final state particles. The distributions which will be presented in this paper are: $(1/\sigma) d\sigma/d(\Delta y_{\gamma\gamma})$, $(1/\sigma) d\sigma/d(\Delta\phi_{\gamma\gamma})$ and $(1/\sigma) d\sigma/dR_{\gamma\gamma}$. The distributions are normalized by the cross section to reduce the sensitivity to Q^2 and differences in parton distributions. The following inputs are used for this calculation: $\sqrt{s} = 1800$ GeV, CTEQ3L parton distributions [2], the one-loop expression for $\alpha_s(Q^2)$, $Q^2 = p_{T\gamma}^2$, and $m_{top} = 180$ GeV. Additionally, unless otherwise stated, the following cuts are used: $p_{T\gamma} > 10$ GeV, $p_{Tjet} > 10$ GeV, $|y_\gamma| < 2.5$, $|y_{jet}| < 3.0$, and $R > 0.4$.

Fig. 1 shows the results for the $\Delta y_{\gamma\gamma}$ distribution. The dashed curve is class (1), dot-dash class (2), dotted class (3), and the solid curve is the sum of the three. It can be seen that the distribution is a rapidly falling function of $\Delta y_{\gamma\gamma}$ and that the three classes are distinct. It should be noted that the separation can be enhanced by requiring a stiffer p_T cut on the photons thus enhancing class (3) events at the cost of reducing the total number of events.

Fig. 2 shows the results for the $\Delta\phi_{\gamma\gamma}$ distribution. This distribution has three distinct features: a “shoulder”, a “double-hump”, and a “bump”. Each is associated with class (1), class (2) and class (3) type events accordingly. The locations of each peak can be understood

easily from the kinematics of each class. In class (1) events both photons have lower p_T than the jet and are thus recoiling against the jet. Therefore class (1) events dominate at low $\Delta\phi_{\gamma\gamma}$. The probability to have a class (1) event increases with $\Delta\phi_{\gamma\gamma}$ until $\Delta\phi_{\gamma\gamma}$ reaches $\frac{\pi}{2}$ and class (2) events “turn on”. The “double-hump” or twin-peak structure of class (2) events can also be understood. In class (2) events the jet p_T is intermediate in the p_T ordering. The probability of class (2) events also increases with $\Delta\phi_{\gamma\gamma}$ to peak at $\frac{2\pi}{3}$. These events are the so-called “Benz” events where each of the final state particles has nearly equal momentum. This is also the location of the “turn on” of class (3) events. Both class (2) and class (3) events are strongly peaked near π . For class (2) events this occurs when one of the photons is soft and in class (3) events when the jet is soft. It is important to remember that although kinematics determines the location of the various peaks, the matrix elements determine the relative heights and shapes of the distributions. Also, as in the $\Delta y_{\gamma\gamma}$ distribution, the separation of the classes can be enhanced by requiring a stiffer p_T cut on the photons thus enhancing class (3) events at the cost of reducing the total number of events.

Fig. 3 shows the results for the $R_{\gamma\gamma}$ distribution. The three classes are once again clearly separated and retain much of the structure shown in the $\Delta\phi_{\gamma\gamma}$ plots. The “shoulder” from class (1) events is clearly visible. The “double-hump” of class (2) events has been smeared out, but the peaking of class (2) and class (3) events at R near three is a remnant of $\Delta\phi_{\gamma\gamma}$ peaking near π . Also, as in the previous distributions, the separation of the classes can be enhanced by requiring a stiffer p_T cut on the photons thus enhancing class (3) events at the cost of reducing the total number of events.

From a experimental point of view it should be noted that the requirements on the jet can be relaxed. In fact the jet need not be directly observed, just inferred from a large p_T imbalance between the photons. This removes the uncertainties associated with jet definitions, jet momentum and jet triggering efficiencies. As mentioned in the text, the various classes of events can be enhanced by adjusting the p_T cut on the photons or the jet. It should also be noted that the photons can be restricted to more central rapidities at the cost of a lower cross section. Finally it should be noted the analysis presented here can be

carried over to the di-jet + photon process (jets and photon must be directly observed).

ACKNOWLEDGMENTS

This research was supported in part by Eckerd College and is a continuation of research that was supported by the U. S. Department of Energy under contract number DE-FG05-87-ER40319. The author would like to thank the Florida State University Department of Physics and Argonne National Laboratory for the use of computer facilities. Additionally, the author would like to thank G. Blazey and J. Womersley for stimulating discussions.

REFERENCES

- [1] S. Keller and J. F. Owens, Phys. Lett. **B269**, 445 (1991).
- [2] CTEQ Collaboration, Phys. Rev. **D51**, 4763 (1995).

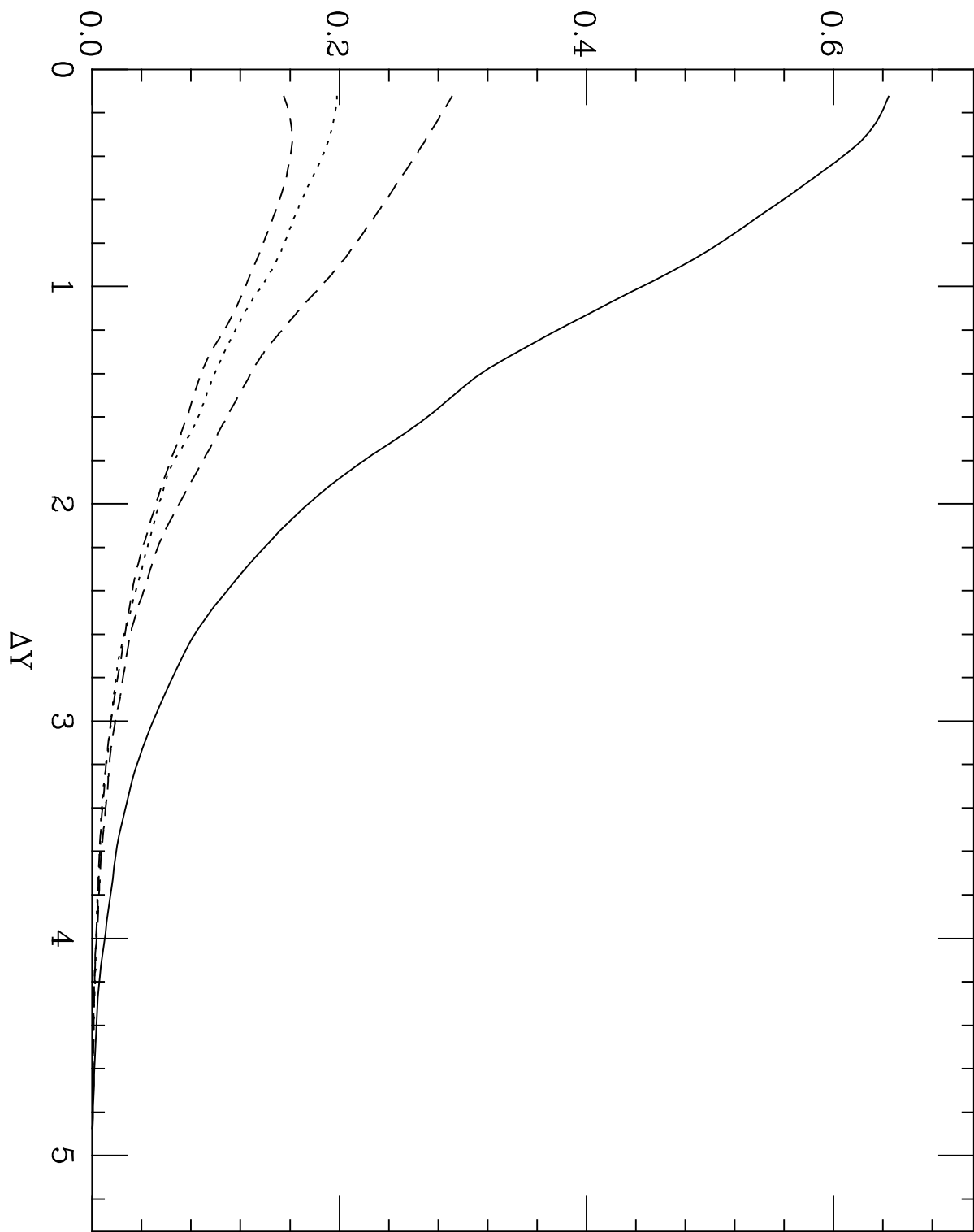
FIGURES

Figure 1. $d\sigma/d(\Delta y_{\gamma\gamma})$ vs. Δy distribution using the cuts described in the text. The dashed curve is class (1), dot-dash curve is class (2), dotted curve is class (3), the solid curve is the sum of the three.

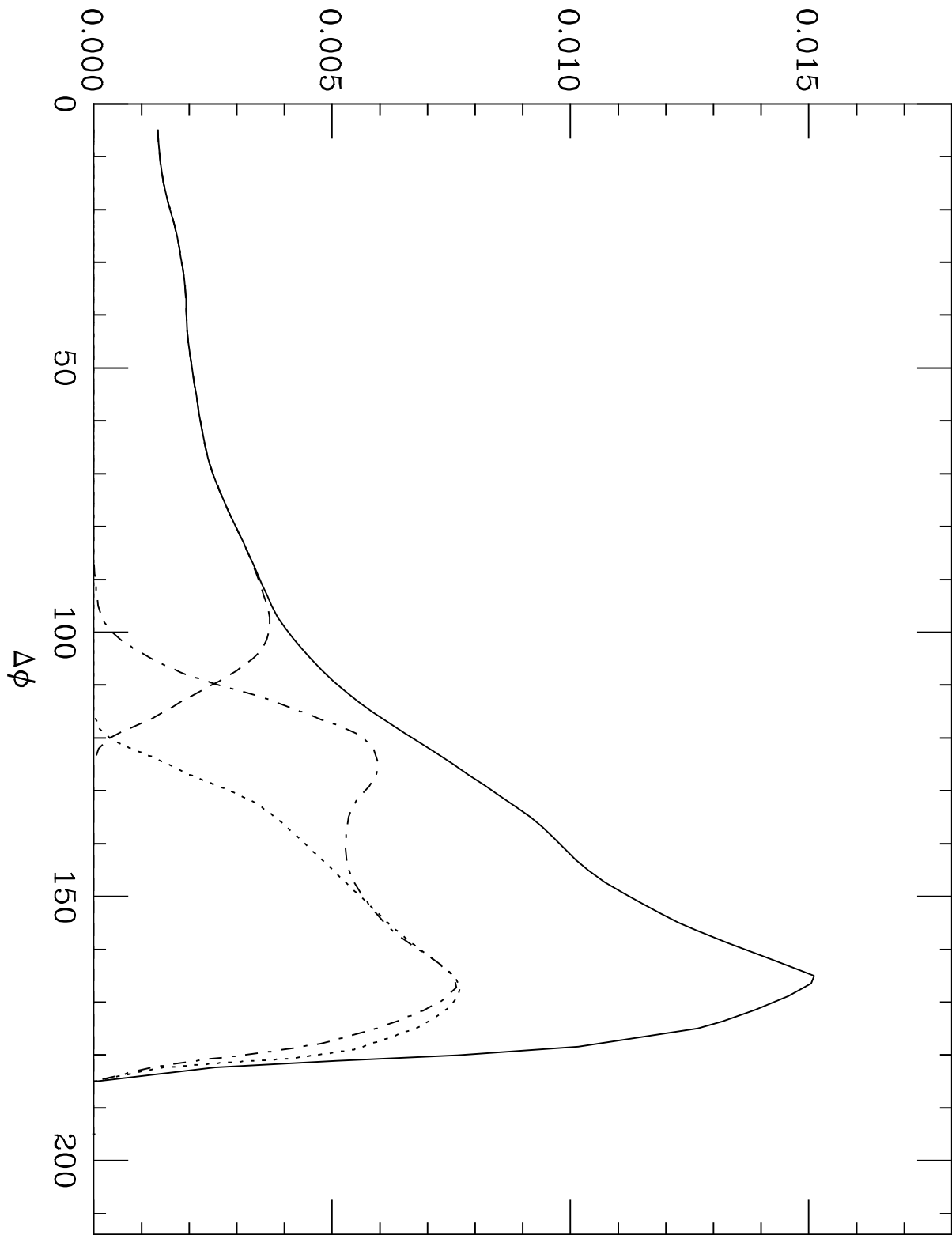
Figure 2. $d\sigma/d(\Delta\phi_{\gamma\gamma})$ vs. $\Delta\phi$ distribution using the cuts described in the text. The dashed curve is class (1), dot-dash curve is class (2), dotted curve is class (3), the solid curve is the sum of the three.

Figure 3. $d\sigma/dR_{\gamma\gamma}$ vs. R distribution using the cuts described in the text. The dashed curve is class (1), dot-dash curve is class (2), dotted curve is class (3), the solid curve is the sum of the three.

$$(1/\sigma) \frac{d\sigma}{d(\Delta Y)}$$



$(1/\sigma) \frac{d\sigma}{d(\Delta\phi)}$



$$(1/\sigma) \frac{d\sigma}{dR}$$

